A desorption mechanism of water following vacuum-ultraviolet irradiation on amorphous solid water at 90 K

Tetsuya Hama,[1,a)] Masaaki Yokoyama,[1] Akihiro Yabushita,[1] Masahiro Kawasaki,[1,b)] Stefan Andersson,[2] Colin M. Western,[3] Michael N. R. Ashfold,[3] Richard N. Dixon,[3] and Naoki Watanabe[4]

[1]*Department of Molecular Engineering, Kyoto University, Kyoto 615-8510, Japan*
[2]*SINTEF Materials and Chemistry, 7465 Trondheim, Norway and Department of Chemistry, Physical Chemistry, University of Gothenburg, 41296 Gothenburg, Sweden*
[3]*School of Chemistry, University of Bristol, Bristol BS8 1TS, United Kingdom*
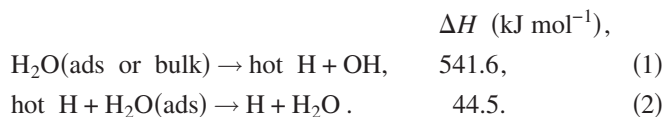[4]*Institute of Low Temperature Science, Hokkaido University, Sapporo 060-0819, Japan*

Following 157 nm photoexcitation of amorphous solid water and polycrystalline water ice, photodesorbed water molecules (H_2O and D_2O), in the ground vibrational state, have been observed using resonance-enhanced multiphoton ionization detection methods. Time-of-flight and rotationally resolved spectra of the photodesorbed water molecules were measured, and the kinetic and internal energy distributions were obtained. The measured energy distributions are in good accord with those predicted by classical molecular dynamics calculations for the kick-out mechanism of a water molecule from the ice surface by a hot hydrogen (deuterium) atom formed by photodissociation of a neighboring water molecule. Desorption of D_2O following 193 nm photoirradiation of a D_2O/H_2S mixed ice was also investigated to provide further direct evidence for the operation of a kick-out mechanism. © *2010 American Institute of Physics*. [doi:10.1063/1.3386577]

I. INTRODUCTION

In interstellar molecular clouds characterized by dense clumps of material and excess vacuum-ultraviolet (vuv) photons, photoirradiation on dust grains induces desorption of molecules. Photodesorption is often invoked to account for the high gas-phase abundances of less volatile molecules, such as water, that are observed under conditions where complete freeze-out onto dust grains might otherwise be expected.[1,2] Given the typical size of dust grain and magnitude of vuv flux inside dense molecular clouds, the arrival rate of vuv photons on a dust grain is estimated to be about one photon per day.[3,4] A proper appreciation of the effects of single UV absorption events is thus likely to be important in developing a realistic picture of photodesorption in dense molecular clouds. Several experimental studies of the photodesorption of water molecules from ice surfaces have been performed.[5–9] Wolf *et al.* studied water molecule desorption following 193 nm ($2-40$ mJ cm^{-2}) irradiation of the water bilayer adsorbed on a Pd(111) surface, which is due to metal substrate excitations, and reported that the photodesorption became inefficient when water multilayers (>4 ML) were adsorbed.[10] Öberg *et al.*[11] used a vuv lamp emitting in the range of 7.0–10.5 eV ($1.1-5.0 \times 10^{13}$ photons cm^{-2} s^{-1}) to irradiate ices at surface temperatures of 18–100 K and detected H_2O, OH, H_2, and O_2 as desorbing species. Molecular dynamics (MD) calculations by Andersson and van Dishoeck[3] proposed a kick-out mechanism for water photodesorption following absorption of a single UV photon, i.e., an H_2O molecule is ejected from the ice by momentum transfer, mainly to the oxygen atom in H_2O, from an energetic H atom released by photodissociation of a neighboring H_2O, i.e., reactions (1) and (2),

$$\Delta H \text{ (kJ mol}^{-1}\text{),}$$

$$H_2O(\text{ads or bulk}) \rightarrow \text{hot } H + OH, \quad 541.6, \quad (1)$$

$$\text{hot } H + H_2O(\text{ads}) \rightarrow H + H_2O. \quad 44.5. \quad (2)$$

In the case of 157 nm ($E_{\text{phot}} = 762.0$ kJ mol^{-1}) photolysis, the excess energy over and above that required for reaction (1), $E_{\text{avail}}(1)$, is 220.4 kJ mol^{-1}. Thermodynamic values are calculated using solid or dilute solution phase thermodynamic data for the condensed or adsorbed water ("ads") and gas-phase data for other species.[12,13] We have previously investigated the photodesorption processes of energetic hydrogen atoms and water molecules from both amorphous solid water (ASW) and polycrystalline water ice (PCI) at 90 K using pulsed 157 or 193 nm laser radiation, i.e., at wavelengths within the first absorption band of the ice, thereby revealing the translational and internal energy distributions of the photodesorbed species.[14–16]

In the present work, we have performed (a) an experimental study of photodesorption mechanisms and dynamics of water molecules from ASW and PCI at 90 K seeking evidence for the operation of the kick-out mechanism, i.e., reaction (2), and (b) classical MD calculations of the translational and rotational energies of photodesorbed H_2O molecules from an ASW ice surface.

II. EXPERIMENTAL

A. Apparatus and preparation of ice

The apparatus has been described before,[17] and only details relevant to the present experiments are given here. A vacuum chamber was evacuated to a base pressure of 10^{-8} Torr using two turbo-molecular pumps in tandem (Shimadzu, 800 and 50 $1\,s^{-1}$). An optically flat sapphire disk substrate, sputter coated with a thin polycrystalline film of Au(111), was supported in the center of the chamber by a liquid-nitrogen-cooled manipulator connected to an X-Y-Z stage.[18] The temperature of the substrate was controlled to within 1 K.

Three types of ice samples were prepared: amorphous solid H_2O and D_2O water ices [henceforth termed ASW(H_2O) and ASW(D_2O), respectively], polycrystalline H_2O water ice (PCI(H_2O)), and a D_2O ice sample containing an H_2S ice interlayer. ASW were prepared by backfilling deposition of water vapor onto the polycrystalline gold substrate at 90 K for 60 min. The chamber pressure was 5 $\times 10^{-7}$ Torr during the deposition. PCI(H_2O) samples were prepared by deposition of background H_2O vapor at 130 K for 60 min and then further maintaining the ice at 130 K for 30 min for annealing purposes. The prepared PCI(H_2O) may have both cubic and hexagonal structures. Its surface is partially disordered due to grain boundaries.[17] Since time-of-flight (TOF) spectra of the photofragment hydrogen atoms following 193 nm photolysis of water molecules on ice surface strongly depend on surface morphology,[14,15] the morphology of the prepared PCI surface was confirmed by observing the TOF spectrum of the photofragment hydrogen atoms. Details of the characteristics of prepared ASW and PCI have been discussed in our previous publications.[14,15,17]

To obtain the nascent internal and kinetic energy distributions of photodesorbed water molecules without the influence of the ice/gold interface, we performed thick-ice-experiments. The water vapor exposure was typically 1500 L (1 $L=1\times10^{-6}$ Torr s). This exposure resulted in formation of roughly 500 ML of H_2O (or D_2O) on the substrate if we adopt the reported experimental conversion factor of 1 ML deposition by 3 L exposure,[19] which are expected to be sufficiently thick to negate the possible influence of reactions at the ice/gold substrate interface and of any photoelectrons from the gold substrate.[10,20–22]

For the $D_2O:H_2S$ mixed ice sample, the ASW(D_2O) was exposed to a mixture of $H_2S(30\%)+N_2(70\%)$ gas. The H_2S exposure was $\sim$80 L for 10 min duration at 90 K. After H_2S deposition, D_2O (10–70 L) was further deposited on the H_2S layer.

Unfocused F_2 excimer laser (Lambda Physik, OPTexPro, Göttingen, Germany) radiation at 157 nm with a pulse duration of 10 ns was incident on the ice surface at an angle of $\sim$80° to the surface normal and at a fluence, $F<0.1$ mJ $cm^{-2}(\sim10^{14}$ photons cm^{-2} pulse$^{-1})$; the corresponding fluence when using an ArF excimer laser (Lambda Physik, COMPex) at 193 nm was $F<1.0$ mJ $cm^{-2}(\sim10^{15}$ photons cm^{-2} pulse$^{-1})$. Although Yabushita *et al.* previously observed hydrogen atom photofragments following 193 nm photodissociation of ASW and PCI,[14,15] 193
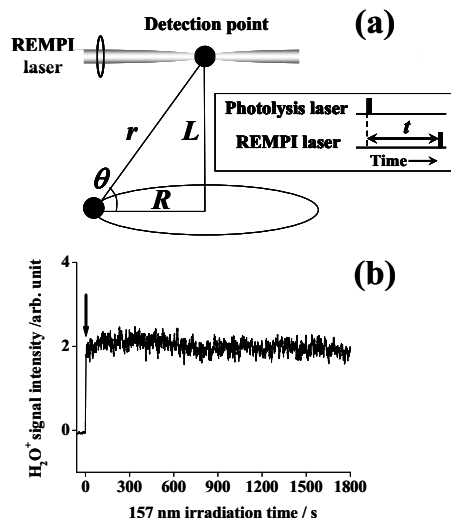

FIG. 1. (a) Schematic illustration of the experiment. Desorbed water molecules following 157 nm photoirradiation on ice samples are detected by the REMPI technique. The timing plot for measurements of a TOF spectrum is also shown where the delay time, t, between photolysis and probe laser pulses corresponds to the TOF. A ellipse indicates an irradiation area on the substrate. $L(=2$ mm) is the vertical distance between the substrate and the detection point. $R(=6$ mm) is the radius of the irradiation area. r is the effective flight distance to the REMPI probe region given by $r=(L^2+R^2)^{1/2}$. θ is the surface polar coordinate. (b) Time evolution curve of the $H_2O(v=0)$ REMPI signal measured via the 2_{02}-3_{21} line of the $C-X$ 0_0^0 transition, as a function of irradiation time at 157 nm at fixed delay $t=2.5$ μs. The arrow indicates the time at which 157 nm irradiation starts.

nm irradiation of ASW(H_2O or D_2O) resulted in no measurable H_2O or D_2O resonance-enhanced multiphoton ionization (REMPI) signal in such thick condensed ice and weak 193 nm laser intensity, which is consistent with the previously reported experimental study by Wolf *et al.*[10]

The photoirradiated area in all cases was a disk of radius 6 mm. As shown in Fig. 1(a), photodesorbed H_2O and D_2O molecules were detected by 2+1 REMPI via the $C(000)$ $-X(000)$ transition, at wavelengths in the range of 247.5–248.5 nm produced by frequency doubling the output of a Nd^{3+}:YAG pumped dye laser (Lambda Physik, SCANmate) and collected with a small mass spectrometer aligned perpendicularly to the ice surface.

B. Simulation of 2+1 REMPI spectra of water molecules

PGOPHER, a program for simulating the rotational structure accompanying one- and multiphoton electronic transitions,[23] was used to simulate the measured 2+1 REMPI spectra and thereby establish best-fit values of the rotational temperatures of the water products. Spectroscopic parameters for the ground and excited state levels of H_2O and D_2O were taken from the literature,[24] including a recent re-examination of the two photon spectra. The simulation included the effect of excited state predissociation, as discussed in the cited works, which gives a predissociation rate that scales broadly with $\langle K_a^2\rangle$, i.e., with the expectation value of square of the rotational angular momentum about the a-axis in the C state level of interest. The simulations only included the origin band of the $C-X$ transition and gave a reasonably good fit to the spectra.

Relatively little information is available on vibrationally excited states of the C state,[25] but given the similar geometry of the Rydberg and ground states of water, we would expect any vibrationally excited states to give the strongest spectra in the same region as the origin band. The good fit to ground state only spectra suggests little vibrational excitation in the H_2O and D_2O products, though we note that Uselman et al.[25] suggested an increasing degree of predissociation for higher C state vibrational states, which would make the states harder to detect for increasing vibrational energy, and our detection method is probably completely insensitive to molecules with a large degree of vibrational or rotational excitation.

The spin temperature was taken to be the same as the rotational temperature for both H_2O and D_2O. There is some discussion (see, for example, Bonev et al.[26]) on the question of whether spin temperatures in comets are always in equilibrium, though note that for all the temperatures used here (>50 K), the ortho:para ratios are essentially the statistical values of 3:1 for H_2O and 2:1 for D_2O. A lower temperature experiment would be necessary to probe any nuclear spin state selectivity.

C. Simulation of TOF spectra of desorbed water molecule

TOF spectra of photoproducts were taken as a function of time, t, between the photolysis and REMPI laser pulses using a delay generator (Stanford Research) in order to investigate the translational energies of the desorbing photoproducts as shown schematically in Fig. 1(a). The measured TOF spectra, $S(t, T_{trans})$, were fitted to a Maxwell–Boltzmann (MB) distribution, S_{MB}, defined by a translational temperature, T_{trans}. Details regarding the simulation of such TOF spectra in terms of Eq. (3) have been reported previously,[17]

$$S_{MB}(t, T_{trans}) = r^3 t^{-4} \exp[- mr^2/2k_B T_{trans}t^2], \qquad (3)$$

where r is the flight distance to the REMPI probe region given by $r = (L^2 + R^2)^{1/2}$ as shown in Fig. 1(a). In these calculations we assume that signals come from a disk (vuv photoirradiation area) with a radius of 6 mm, and the detection probability is proportional to $2\pi R dR/(L^2 + R^2)$, where $L(=2$ mm) is a vertical flight distance and $R(0 \leq R \leq 6$ mm) is the radius of the irradiation area. The MB distribution, $P_{MB}(E_t)$, as a function of translational energy, E_t, is characterized by the averaged translational energy, $\langle E_t \rangle = 2k_B T_{trans}$, where k_B is the Boltzmann constant,[27]

$$P_{MB}(E_t) = (k_B T_{trans})^{-2} E_t \exp[- E_t/k_B T_{trans}]. \qquad (4)$$

Conversion from the E_t distribution to the TOF distribution was performed using the Jacobian given by Zimmerman and Ho.[28] The angular distribution of the molecules photodesorbed from the ice surface was assumed to follow a $\cos^n \theta$ function, where θ is the surface polar coordinate. $n = 0$ was adopted in the best-fitting procedures.[17,29]

D. MD calculation method

All our calculations have been performed using classical MD methods[30] with analytical potentials. Details of the com-

putational procedure have been described in the work of Andersson et al.[3,31] Here, only a brief outline of the methods will be presented.

1. Amorphous water ice

To create an amorphous ice slab, the procedure outlined in the work of Al-Halabi et al.[32] was used. In brief, a slab of eight bilayers (16 monolayers) of crystalline ice was first created consisting of a cell containing 480 molecules. After the transition to amorphous ice, the resulting amorphous ice structure most closely resembles the structure of compact amorphous ice obtained experimentally and is thought to be representative of the structure of interstellar water ice.[31,33]

2. Initial conditions

Once the ice surface is set up, one H_2O molecule is chosen to be photodissociated. This molecule is then made completely flexible, and its intramolecular (internal) interactions are governed by an analytic potential energy surface for the first electronically excited state (the A^1B_1 state) of gas-phase H_2O based on high-quality ab initio electronic structure calculations.[34] This excited potential is fully repulsive so that absorption into this state leads to dissociation of the H_2O molecule into H+OH. Dissociation of molecules in the top three monolayers has been considered. For each monolayer all 30 molecules have been dissociated, one molecule at a time. For each molecule 10 000 configurations and momenta were sampled from a Wigner distribution of the vibrational ground state of H_2O. To reproduce the experimental conditions most closely, only those configurations that correspond to excitation energies in the range of 7.8–8.0 eV (155–159 nm) were chosen as initial conditions for the trajectories. Out of the initial 900000 configurations, about 70000 were in this range and were used for the dynamics calculations.

3. Dynamics of the dissociating molecule

After putting the molecule in the excited state, the dissociating trajectory is integrated with a time step of 0.02 fs. A maximum time of 20 ps has been used before terminating the trajectory. Most of the trajectories (99.5%) were terminated before that because the system was found in one of the final outcomes with negligible probability of transforming into a different state. When the excited H_2O dissociates, the intermolecular interactions are smoothly switched into separate interactions between the photoproducts and water ice, i.e., H–H_2O and OH–H_2O potentials. All details of the potentials and the functions used to switch between different potentials are given in Andersson et al.[31] The switching functions connect the partial charges, the dispersion interactions and repulsive potentials between the H_2O–H_2O potentials and the OH–H_2O and H–H_2O potentials affecting the dissociating molecule.
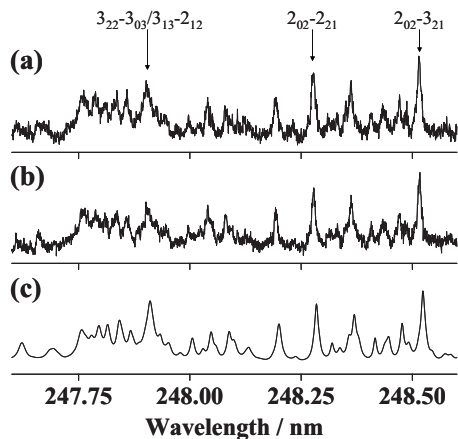
FIG. 2. (a) 2+1 REMPI spectrum of $H_2O(v=0)$ formed by 157 nm photoir-radiation of ASW(H_2O) at 90 K, measured at $t=2.5$ μs. The arrows indicate wavelengths at which TOF spectra were measured for Fig. 3. (b). REMPI spectrum from PCI(H_2O) at 90 K. (c) Simulation of the H_2O, $C-X$, 0_0^0 two-photon spectrum, assuming a Boltzmann rotational state population distribution with $T_{rot}=350$ K and $g_{OPR}=3$.

III. EXPERIMENTAL RESULTS

A. Photodesorption of H_2O following 157 nm photoirradiation of ASW(H_2O)

Figure 2(a) shows a rotationally resolved REMPI spectrum of $H_2O(v=0)$ molecules observed following 157 nm photoirradiation of ASW(H_2O) at 90 K and a fixed delay time, $t=2.5$ μs. The best-fit simulation obtained using the appropriate two-photon rotational line strengths and widths given the previously reported rotational level dependent pre-dissociation of the $C(v=0)$ state is shown in Fig. 2(c). By comparison with spectral simulation, the rotational temperature, T_{rot}, is determined as 350 ± 150 K ($\langle E_{rot}\rangle$ $=4.4\pm1.9$ kJ mol^{-1}) and the ortho:para ratio, g_{OPR}, esti-mated to be 3 [which is the statistical equilibrium value above ~60 K (Ref. 26)].

Figure 3(a) shows a TOF spectrum of $H_2O(v=0)$ mea-sured when exciting the 2_{02}-3_{21} line of the $C-X$ origin band at 248.514 nm, which is reproduced well by a MB distribution with $T_{trans}=1800\pm500$ K ($\langle E_{trans}\rangle$ $=29.9\pm8.3$ kJ mol^{-1}). Changing the probe wavelength to excite other transitions, e.g., the $C-X$, 0_0^0, 2_{02}-2_{21} line or the blended 3_{22}-$3_{03}/3_{13}$-2_{12} lines, caused no discernible change in the TOF profiles. Table I summarizes these results. Figure 1(b) shows the time evolution of the H_2O, $C-X$, 0_0^0, 2_{02}-3_{21} line intensity as a function of duration of the 157 nm irradia-tion. The signal appeared promptly and remained constant during 30 min of subsequent irradiation.

157 nm irradiation of PCI(H_2O) yielded REMPI and TOF spectra of $H_2O(v=0)$ that were essentially identical both in intensity and profile to those obtained from the ASW sample as shown in Figs. 2(b) and 3(b). T_{rot} is estimated to be 350 ± 150 K ($\langle E_{rot}\rangle=4.4\pm1.9$ kJ mol^{-1}) from the REMPI spectrum [Figs. 2(b) and 2(c)], and a TOF spectrum obtained when exciting the 2_{02}-3_{21} line of the REMPI spec-trum is reproduced with $T_{trans}=1600\pm500$ K ($\langle E_{trans}\rangle$ $=26.6\pm8.3$ kJ mol^{-1}) [Fig. 3(b)]. The temporal evolution of
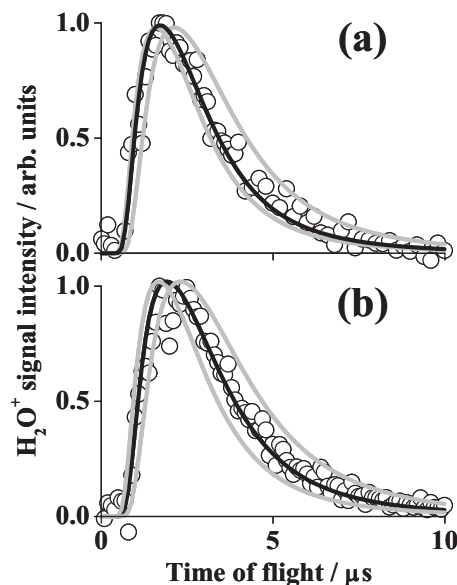

FIG. 3. (a) TOF spectrum of $H_2O(v=0)$ formed by 157 nm photoirradiation of ASW(H_2O) at 90 K, monitored via the 2_{02}-3_{21} line of the $C-X$ 0_0^0 two-photon transition. The solid curve is a fit to the data derived assuming a MB distribution with $T_{trans}=1800$ K. (b) TOF spectrum of $H_2O(v=0)$ from PCI(H_2O) at 90 K, monitored via the same line with the case of ASW(H_2O). The solid curve is a fit to the data derived assuming $T_{trans}=1600$ K. The two gray curves show the range spanned by the error bars quoted in Table I.

the $H_2O(v=0)$ signal intensity was also essentially identical to that shown in Fig. 1(b) for the case of $H_2O(v=0)$ from ASW.

B. Photodesorption of D_2O following 157 nm photoirradiation on ASW(D_2O)

Figure 4(a) shows a rotationally resolved REMPI spec-trum of part of the $C-X$ 0_0^0 transition of D_2O formed by 157 nm photoirradiation on ASW(D_2O) at 90 K and $t=2.5$ μs. The best-fit simulation, which assumes $T_{rot}=350\pm150$ K ($\langle E_{rot}\rangle=4.4\pm1.9$ kJ mol^{-1}) and $g_{OPR}=2$, is shown in Fig. 4(b). Figure 5(a) shows a TOF spectrum of photodesorbed $D_2O(v=0)$ molecules measured when exciting the line at 248.057 nm of the D_2O, $C-X$, 0_0^0 band (of which the largest contributor is 3_{12}-4_{31} transition), which is reproduced well by a MB distribution with $T_{trans}=1800\pm500$ K ($\langle E_{trans}\rangle$ $=29.9\pm8.3$ kJ mol^{-1}). We have also measured TOF spectra for the D_2O line at 247.525 nm for which several lines around $J=10$ contribute. This TOF spectrum was similar to that when exciting the line at 248.057 nm and re-produced well assuming $T_{trans}=2000\pm500$ K ($\langle E_{trans}\rangle$ $=33.3\pm8.3$ kJ mol^{-1}). Table I summarizes these results.

C. Photodesorption of D_2O following 193 nm photoirradiation of capped D_2O:H_2S mixed ice layers

193 nm irradiation of pure ASW(H_2O) or ASW(D_2O) resulted in no measurable H_2O or D_2O REMPI signal. 193 nm irradiation of D_2O:H_2S mixed ice layer does result in $D_2O(v=0)$ molecules, however, as illustrated by the TOF spectrum measured when exciting the REMPI line at 247.865 nm (mainly the 1_{01}-2_{20} transition of the D_2O, $C-X$, 0_0^0 band) as shown in Fig. 5(b). This TOF spectrum is

TABLE I. Translational and rotational temperatures of photodesorbed $H_2O(v=0)$ and $D_2O(v=0)$ from the 157 nm photolysis of ASW at 90 K.

	Temperatures (wavenumbers)	
	Translation	Rotation
H_2O from H_2O amorphous solid water[a]	1800 ± 500 K (2502 ± 695 cm^{-1})	350 ± 150 K (243 ± 104 cm^{-1}) [b]
D_2O from D_2O amorphous solid water[a]	1800 ± 500 K (2502 ± 695 cm^{-1})	350 ± 150 K (243 ± 104 cm^{-1}) [b]
D_2O from D_2O:H_2S mixed ice layer[c]	2250 ± 750 K (3128 ± 1043 cm^{-1})	... [d]
MD calculation	1450 ± 150 K (2016 ± 209 cm^{-1})	300 ± 50 K (209 ± 35 cm^{-1})

[a]157 nm photoirradiation.
[b]From spectra recorded at $t=2.5$ μs.
[c]193 nm photoirradiation.
[d]Not measured.

reproduced well with $T_{trans}=2250 \pm 750$ K ($\langle E_{trans} \rangle =37.4 \pm 12.5$ kJ mol^{-1}). The formation of these $D_2O(v=0)$ is assumed to involve initial formation of translationally hot H atoms by 193 nm photolysis of H_2S, which induce the subsequent photodesorption of D_2O via the kick-out mechanism. The coverage dependence of the REMPI signal intensity was measured as a function of the dose rate in the range of 10–70 L used to deposit the top D_2O layer. Stronger D_2O signals were observed for thicker top D_2O layers presumably because the lower D_2O exposures did not result in perfectly coverage of the H_2S underlayer. The incomplete coverage was previously obtained in the 193 nm photolysis of H_2O/D_2O ice systems, i.e., 30 L exposure of H_2O vapor could cover only the top most D_2O surface layer of the ASW(D_2O) because of the surface roughness.[14]

We were not able to characterize the rotationally resolved REMPI spectrum for the D_2O molecules as the signal intensity declined steadily during the scan—presumably as a result of depletion of the H_2S and thus of H atoms to induce the kick-out process upon prolonged exposure to 193 nm irradiation.

IV. MD RESULTS

Details of the MD results of photodesorption following photoexcitation of water ice are described by Andersson *et al.*;[3,31] here only details relevant to H_2O desorption will be presented. Photodissociation of a water ice molecule can
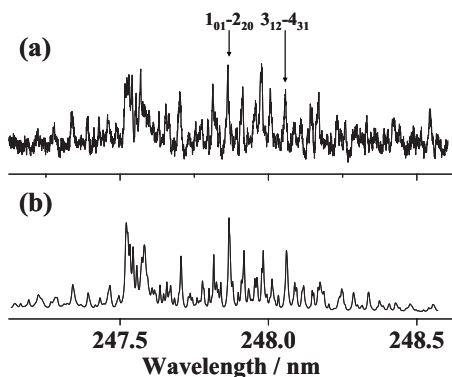
have several outcomes, with the H and OH photoproducts either becoming trapped in the ice, recombining back to a H_2O molecule, or desorbing from the ice surface. The probability of photodesorption of H_2O is seen to be low, 1.2% and 0.8% per absorbed UV photon in the first and second monolayers, respectively, and then decreases with distance from the surface. Analysis of the trajectories shows that there are two distinct mechanisms for the removal of H_2O molecules: (a) *Kick-out mechanism*, an H atom released from photodissociation of H_2O is able to transfer enough momentum to one of the other H_2O molecules to kick it off the surface and (b) H+OH *recombination mechanism*, H and OH promptly recombine to form H_2O and subsequently desorb. In the top two monolayers, both the kick-out and the H +OH recombination mechanisms occur with relative probability ratios of one to four. When photoexcitation occurs in
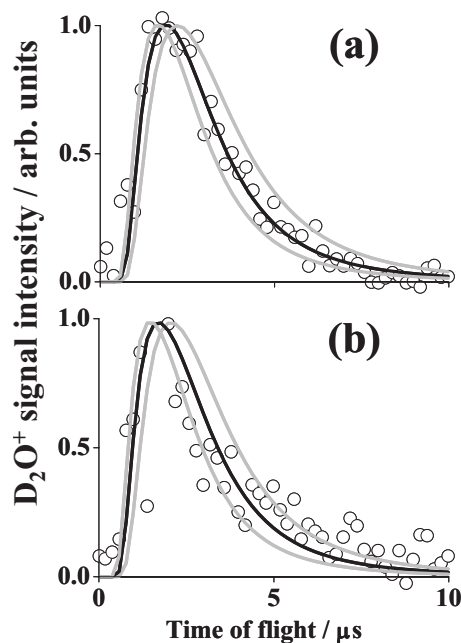

FIG. 4. (a). 2+1 REMPI spectrum of $D_2O(v=0)$ formed by the 157 nm photoirradiation of ASW(D_2O) at 90 K, measured at $t=2.5$ μs. (b). Simulation of the D_2O, $C-X$, 0_0^0 two-photon spectrum, assuming a Boltzmann rotational state population distribution with $T_{rot}=300$ K and $g_{OPR}=2$. The arrows indicate wavelengths at which TOF spectra were measured for Fig. 5.

FIG. 5. (a) TOF spectrum of $D_2O(v=0)$ formed by 157 nm photoirradiation of ASW(D_2O) at 90 K, monitored by 2+1 REMPI via the line at 248.057 nm of the $C-X$ 0_0^0 band. The solid curve is a fit to the data derived assuming $T_{trans}=1800$ K. (b) TOF spectrum of $D_2O(v=0)$ formed by 193 nm photoirradiation of the D_2O:H_2S mixed ice sample at 90 K, monitored by (2+1) REMPI via the line at 247.865 nm, which is mainly the 1_{01}-2_{20} transition of the $C-X$ 0_0^0 band. The solid curve is a fit to the data derived assuming $T_{trans}=2250$ K. The two gray curves show the range spanned by the error bars quoted in Table I.

the third monolayer, the total H_2O desorption probability is 0.4%, and here the kick-out mechanism is dominant, four times more likely than the other mechanism. Because the H_2O molecules are restricted to be rigid, they are by construct considered to be in their vibrational ground states. The recombination process results in the formation of vibrationally excited H_2O molecules, with an average rovibrational energy almost exactly equal to the dissociation limit of H_2O. This should be seen as an upper limit, since the present MD model does not allow energy transfer to the vibrational modes of the surrounding molecules. The lowest calculated rovibrational energy is 173.7 kJ mol^{-1} above the zero-point energy level. Thus, there was no evidence of desorption of H_2O in the vibrational ground state from the recombination mechanism. We could not observe vibrationally excited H_2O experimentally because of spectroscopic limitations. The calculated average translational and rotational energies of $H_2O(v=0)$ for the kick-out mechanism is $T_{\text{trans}}=1450\pm150$ K ($\langle E_{\text{trans}}\rangle=24.1\pm2.9$ kJ mol^{-1}) and $T_{\text{rot}}=300\pm50$ K ($\langle E_{\text{rot}}\rangle=3.7\pm0.6$ kJ mol^{-1}), respectively. These values are in good accord with the experimental values as shown in Table I.

One interesting observation regarding molecules desorbing via the kick-out mechanism is that their translational energies are much higher than the rotational energies. The likely explanation for this is that the H atom dissociates along the hydrogen bond connecting it to the neighboring H_2O molecule. It thereby hits the O atom and not one of the H atoms, which could lead to (a) reaction or (b) high rotational excitation. Because the H atom hits the H_2O molecule close to the center of mass, most of the energy is transferred into translation and much less into rotation. Hitting the O atom in the H_2O molecule also gives rise to an intermediate H_3O configuration that redissociates into H and H_2O and not to H_2+OH. In the experiments by Yabushita *et al.*,[35,36] photodesorbing H_2 molecules were observed, which were inferred to be produced from the reaction of H atoms with H_2O molecules. Because the H_2O molecules are restricted to be rigid in the MD simulations, it is at present not possible to study this reaction.

V. DISCUSSION

A. Dependence on water ice morphology

Yabushita *et al.* previously investigated the photodissociation dynamics of ASW and PCI by analyzing the TOF spectra of photofragment hydrogen atoms following 157 and 193 nm photolysis of the water ice.[14,15] For ASW, the translational energy of most H atoms was accommodated to the substrate temperature by collisions with bulk water ice before desorption since ASW has a large surface area with micropores. For PCI, on the other hand, the translationally hot H photofragments could desorb from the surface without losing energy by collisions with PCI. However, the present H_2O measurements show little difference in signal intensity or TOF profile when using ASW or PCI samples. This observation suggests that any H_2O molecules that initially desorbed from within the micropores of an ASW sample suffer subsequent collisions with the inside wall of the pore and

readsorb strongly—by hydrogen bonding with the low temperature surface. As a result, only the translationally hot TOF component that escapes without energy loss through interactions with the internal surface of the voids, i.e., primarily from the top surface of the ASW sample, is observed. Since the effective surface area of the uppermost part of the irradiated sample will be similar for both PCI and ASW, it follows that the REMPI and TOF spectra and the time evolution of the desorbed signal intensity should be similar for ASW and PCI. Even if hot water molecules are produced deep within the bulk phase, they cannot come out to the vacuum as suggested by the MD calculation.[3,31] Similar behaviors were observed in desorption of OH radicals and $O(^1D_2$ and $^3P_J)$ atoms following 157 nm photoirradiation of water ice, i.e., the dominant fraction of OH and $O(^1D_2$ and $^3P_J)$ products desorbed into vacuum is released from the surface of water ice.[37–39]

### B. Desorption mechanisms of $H_2O(v=0)$

We have previously discussed four possible desorption mechanisms under 157 nm photoirradiation.[16]

(a) *Kick-out mechanism*: An H atom released by photodissociation of H_2O in the ice transfers enough momentum to another H_2O molecule to cause its ejection from the ice surface.

(b) H+OH *recombination mechanism*: The recombination of photoproduced H and OH species to reform H_2O is highly exothermic ($\Delta H=-497.1$ kJ mol^{-1}) and sufficient to enable subsequent desorption.[3,31]

(c) *Exciton-mediated mechanism*: Photodesorption associated with excitons in ASW enables transfer of energy from the bulk to near the ice surface and subsequent loss of molecules from the surface.[40,41] The lowest energy electronic excitation of H_2O has a threshold at ~725 kJ mol^{-1} ($\lambda \sim 165$ nm).

(d) *Reactions of radicals formed by the photodissociation of ice*: The accumulation and diffusion of photoproduced radicals in, or on, the ice are necessary for water desorption to occur as proposed by Westley *et al.*[7,8]

Photodesorption mechanisms (b) and (c) are both highly exothermic and can be expected to yield vibrationally hot water molecules. As such, we consider them to be unlikely sources for the $H_2O(v=0)$ ejection observed in the present experiments. Furthermore, Fig. 1(b) shows that the $H_2O(v=0)$ desorption from ASW(H_2O) appears promptly after 157 nm irradiation starts, and the desorption yield is independent of 157 nm irradiation time, i.e., the desorption appears to occur without any initial accumulation of photoproduct radicals on the ice surface; hence, mechanism (d) also seems inappropriate. Thus the main photodesorption mechanism for forming $H_2O(v=0)$ products under the present experimental conditions is likely to be the kick-out mechanism (a), i.e., reaction sequences (1) and (2). Hereafter we concentrate discussion on this kick-out mechanism.

1. H₂O *signal intensity change as a function of 157 nm photoirradiation time*

The kick-out mechanism can explain the results shown in Fig. 1(b) since the hot H atom is immediately produced after 157 nm photodissociation of ASW and the concentration of hot H atoms should be stable on/in ASW after each 157 nm laser pulse. Yabushita *et al.* previously observed that the majority of hot H atoms produced by 157 nm photolysis are accommodated by collisions with the ASW sample.[14,15] The subsequent formation of H_2 products via a hydrogen abstraction reaction was also observed with the same experimental setup.[35,36] H_2 formation by reaction sequence (1)–(5) is an endothermic process, and the activation energy for reaction (5) is estimated to be 132.8 kJ mol⁻¹ from the corresponding gas-phase reaction,[42] but the reaction can proceed by virtue of the translational excitation of the hot H atoms formed in the photolysis reaction (1),[15,35,36]

$$\Delta H \ \ (\text{kJ mol}^{-1})$$
$$\text{hot } H + H_2O(\text{ads}) \rightarrow OH + H_2, \quad 107.3. \qquad (5)$$
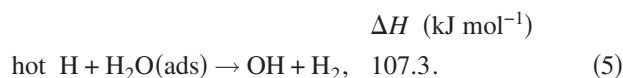
Since the kick-out process (a), i.e., reactions (1) and (2), is less endothermic than H_2 formation by reaction sequence (1)–(5), the H_2O molecules hit by H atoms on the ice surface are likely to be desorbed into vacuum.

In contrast, the H+OH recombination process and the reaction of radicals formed by the photodissociation of ice, mechanisms (b) and (d), both depend on radical accumulation at the surface, and their increasing concentration with irradiation time should thus reveal itself by a progressive increase in desorption rate. Indeed, such behavior has been observed for both OH radicals and O atoms that photodesorb via reactions involving radicals.[37–39] The results shown in Fig. 1(b) thus suggest that mechanisms (b) and (d) are unlikely to be major sources for desorbed $H_2O(v=0)$ molecules.

2. *193 nm photoirradiation experiments for* D₂O:H₂S *mixed ice*

The results of the 193 nm photolysis of the D_2O:H_2S mixed ice layers provides further evidence in support of the kick-out mechanism, i.e., reaction (2). The available energy following S–H bond fission in the gas-phase photolysis of H_2S at 193 nm is $E_{\text{avail}}=238.4$ kJ mol⁻¹.[13] Khriachtchev *et al.*[43] investigated the 193 nm photolysis of H_2S in solid rare-gas matrices and deduced that (as in the gas phase) this excess energy is largely channeled into H atom translational energy.

H_2O or D_2O REMPI signals were not observed in the 193 nm laser irradiation of neat ASW(H_2O) or ASW(D_2O) consistent with the negligible absorption cross-section of bulk ice at this wavelength. H(D) atoms are formed however, but these are attributed to 193 nm photodissociation of dimerlike H_2O or D_2O structures located at the ice/vacuum interface.[14,15,44] Given that they originate from loosely surface-bound species, it is much less likely for such H atoms to induce secondary reactions with neighboring atoms or molecules. Substrate-mediated photodesorption due to the temporary attachment of photo-electrons from the Au substrate is not considered to be a viable mechanism for the present photodesorption of water molecules from the ice surface.[10,22]

C. Other desorption mechanisms for possible formation of H₂O($v \geq 1$)

The present work strongly suggests that kick-out is the dominant desorption mechanism for $H_2O(v=0)$ and $D_2O(v=0)$ molecules following 157 nm photodesorption of ice at 90 K. The present experiments do not exclude the possible formation of vibrationally excited water molecules, however. As argued above, vibrationally excited H_2O molecules might be expected from alternative desorption mechanisms, e.g., the H and OH recombination process (b), or an exciton mediated process (c). We tried to search for REMPI signals of $H_2O(v \geq 1)$, but no evidence for $H_2O(v \geq 1)$ products was obtained, most likely reflecting the limitations of the spectroscopy used. Hence, the other desorption mechanisms will be briefly discussed in the context of possible photodesorption of vibrationally excited $H_2O(D_2O)$ molecules.

1. *H and OH recombination process*

The MD calculations suggest that H atoms could also recombine with OH radicals, and the resulting H_2O molecule subsequent desorb as the recombination is highly exothermic.[3,31] The vuv photolysis studies of Yabushita *et al.*[35,36] deduced that H_2 formation at a water ice surface at 90 K was attributable to the highly exothermic recombination of photolytically produced H atoms. H_2O_2 formation on a water ice surface has also been observed[45] presumably from the recombination of photolytically produced OH radicals. These results serve to encourage the view that photoirradiation leads to desorption of H_2O molecules in excited vibrational levels via the H+OH recombination mechanism.

2. *An exciton-mediated process*

The optical depth of ASW at 157 nm is ~100 nm,[41] so the photon energy available for reaction is primarily absorbed in the bulk of the water ice. A qualitative depiction of the band structure of ice has been reported by Kimmel *et al.*[46] Excitons associated with the $4a_1^* \leftarrow 1b_1$ transition in condensed water have been implicated in a low-energy electron stimulated reaction, which could enable transfer of energy from the bulk to near the ASW surface.[40,41] Kimmel and co-workers found experimental support for the concept of mobile excitons in ASW that initiate reactions at the ASW/vacuum interface.[20,21,47,48] Significant vibrational excitation might be anticipated if the excess energy from the electronic excitation was deposited into an H_2O molecule that desorbed as a result of such a mechanism.

VI. SUMMARY

The translational and rotational energies of water molecules (H_2O and D_2O, in their ground vibrational state) desorbed following 157 nm excitation of amorphous solid water and polycrystalline ice have been measured. The measured energy distributions are in good accord with those

predicted by classical molecular dynamics calculations for the kick-out mechanism, i.e., the ejection of a water molecule from the ice surface by a hot hydrogen (deuterium) atom formed by photodissociation of a neighboring water molecule. Desorption of D_2O following 193 nm photoirradiation of a D_2O/H_2S mixed ice was investigated also for additional direct evidence of the operation of the kick-out mechanism. The ortho:para ratios of the photodesorbed H_2O and D_2O products (3:1 and 2:1, respectively) are appropriate for the measured Boltzmann rotational distributions.

ACKNOWLEDGMENTS

[1] C. Dominik, C. Ceccarelli, D. Hollenbach, and M. Kaufman, Astrophys. J. **635**, L85 (2005).

[2] D. Hollenbach, M. J. Kaufman, E. A. Bergin, and G. J. Melnick, Astrophys. J. **690**, 1497 (2009).

[3] S. Andersson and E. F. van Dishoeck, Astron. Astrophys. **491**, 907 (2008).

[4] C. Shen, J. M. Greenberg, W. A. Schutte, and E. F. van Dishoeck, Astron. Astrophys. **415**, 203 (2004).

[5] J. D. Thrower, D. J. Burke, M. P. Collings, A. Dawes, P. D. Holtom, F. Jamme, P. Kendall, W. A. Brown, I. P. Clark, H. J. Fraser, M. R. S. McCoustra, N. J. Mason, and A. W. Parker, Astrophys. J. **673**, 1233 (2008).

[6] J. D. Thrower, M. P. Collings, M. R. S. McCoustra, D. J. Burke, W. A. Brown, A. Dawes, P. D. Holtom, P. Kendall, N. J. Mason, F. Jamme, H. J. Fraser, I. P. Clark, and A. W. Parker, J. Vac. Sci. Technol. A **26**, 919 (2008).

[7] M. S. Westley, R. A. Baragiola, R. E. Johnson, and G. A. Baratta, Nature (London) **373**, 405 (1995).

[8] M. S. Westley, R. A. Baragiola, R. E. Johnson, and G. A. Baratta, Planet. Space Sci. **43**, 1311 (1995).

[9] J. Bergeld and D. Chakarov, J. Chem. Phys. **125**, 141103 (2006).

[10] M. Wolf, S. Nettesheim, J. M. White, E. Hasselbrink, and G. Ertl, J. Chem. Phys. **94**, 4609 (1991).

[11] K. I. Öberg, H. Linnartz, R. Visser, and E. F. van Dishoeck, Astrophys. J. **693**, 1209 (2009).

[12] M. Kh. Karapet'yants and M. K. Karapet'yants, *Handbook of Thermodynamic Constants of Inorganic and Organic Compounds* (Ann Arbor-Humphrey Science, London, 1970).

[13] S. P. Sander, B. J. Finlayson-Pitts, R. R. Friedl, D. M. Golden, R. E. Huie, H. Keller-Rudek, C. E. Kolb, M. J. Kurylo, M. J. Molina, G. K. Moortgat, V. L. Orkin, A. R. Ravishankara, and P. H. Wine, "Chemical kinetics and photochemical data for use in atmospheric studies, evaluation number 15," JPL Publication 06-2, Jet Propulsion Laboratory, Pasadena, 2006.

[14] A. Yabushita, Y. Hashikawa, A. Ikeda, M. Kawasaki, and H. Tachikawa, J. Chem. Phys. **120**, 5463 (2004).

[15] A. Yabushita, D. Kanda, N. Kawanaka, M. Kawasaki, and M. N. R. Ashfold, J. Chem. Phys. **125**, 133406 (2006).

[16] A. Yabushita, T. Hama, M. Yokoyama, M. Kawasaki, S. Andersson, R. N. Dixon, M. N. R. Ashfold, and N. Watanabe, Astrophys. J. **699**, L80 (2009).

[17] A. Yabushita, Y. Inoue, T. Senga, M. Kawasaki, and S. Sato, J. Phys. Chem. B **106**, 3151 (2002).

[18] M. Kawasaki, Appl. Surf. Sci. **135**, 115 (1998).

[19] S. Sato, D. Yamaguchi, K. Nakagawa, Y. Inoue, A. Yabushita, and M. Kawasaki, Langmuir **16**, 9533 (2000).

[20] N. G. Petrik and G. A. Kimmel, J. Phys. Chem. C **113**, 4451 (2009).

[21] N. G. Petrik, A. G. Kavetsky, and G. A. Kimmel, J. Chem. Phys. **125**, 124702 (2006).

[22] E. H. G. Backus, M. L. Grecea, A. W. Kleyn, and M. Bonn, J. Phys. Chem. B **111**, 6141 (2007).

[23] C. M. Western, PGOPHER, a program for simulating rotational structure, University of Bristol, available at http://pgopher.chm.bris.ac.uk.

[24] M. N. R. Ashfold, J. M. Bayley, R. N. Dixon, and J. D. Prince, Ber. Bunsenges. Phys. Chem. **89**, 254 (1985), and references therein.

[25] B. W. Uselman, J. M. Boyle, and S. L. Anderson, Chem. Phys. Lett. **440**, 171 (2007).

[26] B. P. Bonev, M. J. Mumma, G. L. Villanueva, M. A. Disanti, R. S. Ellis, K. Magee-Sauer, and N. Dello Russo, Astrophys. J. **661**, L97 (2007).

[27] F. M. Zimmermann and W. Ho, J. Chem. Phys. **100**, 7700 (1994).

[28] F. M. Zimmermann and W. Ho, Surf. Sci. Rep. **22**, 127 (1995).

[29] A. Yabushita, Y. Inoue, T. Senga, M. Kawasaki, and S. Sato, J. Phys. Chem. A **108**, 438 (2004).

[30] M. P. Allen and D. J. Tildesley, *Computer Simulations of Liquids* (Clarendon, Oxford, 1987).

[31] S. Andersson, A. Al-Halabi, G.-J. Kroes, and E. F. van Dishoeck, J. Chem. Phys. **124**, 064715 (2006).

[32] A. Al-Halabi, E. F. van Dishoeck, and G. J. Kroes, J. Chem. Phys. **120**, 3358 (2004).

[33] A. Al-Halabi, H. F. Fraser, G. J. Kroes, and E. F. van Dishoeck, Astron. Astrophys. **422**, 777 (2004).

[34] A. J. Dobbyn and P. J. Knowles, Mol. Phys. **91**, 1107 (1997).

[35] A. Yabushita, T. Hama, D. Iida, N. Kawanaka, M. Kawasaki, N. Watanabe, M. N. R. Ashfold, and H.-P. Loock, Astrophys. J. **682**, L69 (2008).

[36] A. Yabushita, T. Hama, D. Iida, N. Kawanaka, M. Kawasaki, N. Watanabe, M. N. R. Ashfold, and H.-P. Loock, J. Chem. Phys. **129**, 044501 (2008).

[37] T. Hama, A. Yabushita, M. Yokoyama, M. Kawasaki, and S. Andersson, J. Chem. Phys. **131**, 054508 (2009).

[38] T. Hama, A. Yabushita, M. Yokoyama, M. Kawasaki, and N. Watanabe, J. Chem. Phys. **131**, 114510 (2009).

[39] T. Hama, A. Yabushita, M. Yokoyama, M. Kawasaki, and N. Watanabe, J. Chem. Phys. **131**, 114511 (2009).

[40] T. M. Orlando and G. A. Kimmel, Surf. Sci. **390**, 79 (1997).

[41] K. Kobayashi, J. Phys. Chem. **87**, 4317 (1983).

[42] D. H. Zhang and J. C. Light, J. Chem. Phys. **104**, 4544 (1996).

[43] L. Khriachtchev, M. Pettersson, E. Isoniemi, and M. Räsänen, J. Chem. Phys. **108**, 5747 (1998).

[44] G. Avila, G. J. Kroes, and M. C. van Hemert, J. Chem. Phys. **128**, 144313 (2008).

[45] A. Yabushita, T. Hama, D. Iida, and M. Kawasaki, J. Chem. Phys. **129**, 014709 (2008).

[46] G. A. Kimmel, T. M. Orlando, C. Vezina, and L. Sanche, J. Chem. Phys. **101**, 3282 (1994).

[47] N. G. Petrik and G. A. Kimmel, Phys. Rev. Lett. **90**, 166102 (2003).

[48] N. G. Petrik and G. A. Kimmel, J. Chem. Phys. **121**, 3736 (2004).